Compton scattering, positron annihilation, and the electronic properties of quantum dots

R. Saniz
Departamento de Ciencias Exactas, Universidad Católica Boliviana, Casilla #5381, Cochabamba, Bolivia

B. Barbiellini
Physics Department, Northeastern University, Boston, Massachusetts 02115

A. Denison*
Idaho National Engineering and Environmental Laboratory, 525 Fremont Avenue, Idaho Falls, Idaho 83415
(Received 7 February 2002; published 11 June 2002)

In this work we study electronic properties of quantum dots relevant to Compton scattering and positron annihilation. The system is modeled by an electron gas confined by a spherical potential of given radius and depth. Electron-electron correlations are not considered in this study. We find that the broadening of the electronic momentum density around a suitably defined Fermi momentum scales with dot radius as $1/R$. The Compton profiles tend to the homogeneous electron gas (HEG) form for high electron densities and large dot radius. The broadening of the electron-positron annihilation probability as a function of total momentum also scales as $1/R$, but the positron increases the broadening by around 20% with respect to the electronic momentum density result. The Doppler profiles deviate more noticeably from the HEG form for small radius and low electron densities. This is reflected well in the Doppler profile shape parameter. Also, positron lifetimes are quite sensitive to electron density and dot radius. Positron lifetimes were calculated taking into account positron-electron correlation through the local-density approximation and the generalized gradient approximation. Within these approximations, the positron lifetime dependence on radius is not monotonic. For large radii, the lifetimes increase with radius toward the HEG values, converging more rapidly for higher electron densities. For a radius smaller than a certain value, however, the lifetime does not continue decreasing with radius but starts to increase, reflecting the increasing spillout of the positron from the dot.

DOI: 10.1103/PhysRevB.65.245310 PACS number(s): 73.22.Dj, 78.67.Hc, 78.70.Bj

I. INTRODUCTION

Interest in quantum dots has continued to increase in the past few years, fueled by the prospects of an ever increasing range of applications. Indeed, to the promising progress already made toward, e.g., optical devices, quantum communications, and quantum computing,[1] one can now add the recent advances toward biological imaging and cell biology studies.[2] Needless to say, a thorough understanding of the physical and chemical properties of these systems is of paramount importance for further progress in related fields. To this end, the study of a quantum dot's electronic properties is of central interest because of the key role these play in determining its overall properties, and many efforts have been made in this direction.[3] In this regard, Compton scattering and positron annihilation have long been known as powerful experimental techniques, yielding complementary information in many respects.[4,5] Positron annihilation, for instance, is being used with great success to investigate different nanostructured systems, like vacancies and embedded particles.[6,7] The distinctive feature of positron annihilation is that in many cases the positron wave function can select the interesting regions of a system due to its repulsion with the nuclei. It is hence of interest to consider the use of these techniques in the study of quantum dots specifically.

In Compton scattering, measuring the energy and angular distribution of scattered radiation yields what is known as a Compton profile, giving us information on the (ground-state) electronic momentum distribution of the system under study. Of particular interest is the so-called momentum broadening, which in crystals measures the width of the region over which the momentum density of valence electrons falls to zero around the Fermi momentum, and which is directly related to the so-called HOMO-LUMO gap (from the chemists' highest occupied molecular-orbital–lowest unoccupied molecular-orbital gap).[8] This gap plays a fundamental role in important optical properties, such as fluorescence. It is thus important to know the characteristics of quantum dots from this point of view. In positron annihilation, on the other hand, two of the basic measurements that can be made are the so-called Doppler profile and the positron lifetime. The shape of the Doppler profile can be characterized in terms of a shape parameter S, which measures the fraction of annihilations within a certain momentum range. Since annihilation probability is expected to change with dot size and electronic density, this must be reflected in the value of the shape parameter. The same observation applies, of course, to positron lifetimes. Actually, Compton scattering can be viewed as a limiting case of positron scattering, namely when the positron wave function can be considered constant. This can be understood from the fact that the scattering cross section is represented essentially by the same Feynman diagram in both cases, albeit Compton scattering involves an electron only.[9] Thus it is of interest to study both techniques at the same time. Theoretical studies of Compton scattering or positron annihilation in quantum dots, however, do not appear to have been presented previously. Because an interpretation of experiment based solely on bulk matter results will undoubt-

edly be of limited value, even qualitatively, it is important to count on the light shed by, at least, a model calculation on these matters. In this work we study the predictions of a simple quantum dot model regarding the quantities discussed above, namely that of an electron gas confined by a spherical potential well of given radius and constant depth. We address, in particular, the effect of dot size and electronic density on the properties studied. In the case of positron lifetimes, electron-positron correlation is taken into account through some approximations.

This paper is organized as follows. In Sec. II we present our model and recall the definitions of the quantities studied. Section III is devoted to presenting and discussing our results. Finally, Sec. IV summarizes our main conclusions.

II. THEORY

As indicated in the Introduction, the quantum dot electron system is represented by an electron gas confined by a potential of the form $V(r)=-V_0, r<R$ and $V(r)=0$ otherwise. Solving the Schrödinger equation for an electron in such a potential yields the single-particle energies and wave functions. The latter are written

$$\varphi_{nlm}(r,\theta,\phi)=Y_{lm}(\theta,\phi)\times\begin{cases}A_{nl}j_l(\kappa_{nl}r), & r<R\\ D_{nl}k_l(\tilde{\kappa}_{nl}r), & r\geqslant R,\end{cases} \tag{1}$$

where the j_l are the spherical Bessel functions of the first kind and the k_l denote here the modified spherical Bessel functions of the third kind,[10] with $\kappa_{nl}^2=2m(\epsilon_{nl}+V_0)/\hbar^2$ and $\tilde{\kappa}_{nl}^2=-2m\epsilon_{nl}/\hbar^2$. The energy levels ϵ_{nl}, $l=0,1,2,\ldots,l_{\max}$, $n=1,2,\ldots,n_l$ are the roots of the eigenvalue equation

$$\tilde{\kappa}j_l(\kappa R)k_l'(\tilde{\kappa}R)-\kappa j_l'(\kappa R)k_l(\tilde{\kappa}R)=0 \tag{2}$$

resulting from the wave function continuity conditions at the dot surface. The normalization constants are given by $A_{nl}=\{2\epsilon_{nl}/[R^3V_0 j_{l+1}(\kappa_{nl}R)j_{l-1}(\kappa_{nl}R)]\}^{1/2}$ and $D_{nl}=A_{nl}j_l(\kappa_{nl}R)/k_l(\tilde{\kappa}_{nl}R)$. If the potential well depth is too shallow, such that $\kappa R\lesssim\pi/2$, then there are no bound solutions. To give an idea of the dependence of the energy levels on n and l, we consider the case $\kappa R\lesssim 8\pi$.[11] We plot them in Fig. 1. The energy level structure is quite typical, showing the same pattern for other radii and well depths. On the right-hand side of Fig. 1 we show the energy levels in a column. Clearly, the level spacing can be very small on the scale of V_0, many levels being quasidegenerate. Level splitting due to, e.g., exchange interaction can make the spectrum even more intriguing. This could be relevant to the energy-level splitting found recently in metallic nanoparticles.[12]

A. Compton scattering

In Compton scattering one measures the intensity of scattered photons in the deep inelastic regime, using either γ or x rays as the primary photon source. A basic quantity in these experiments is the electronic momentum density, which is quite generally defined by

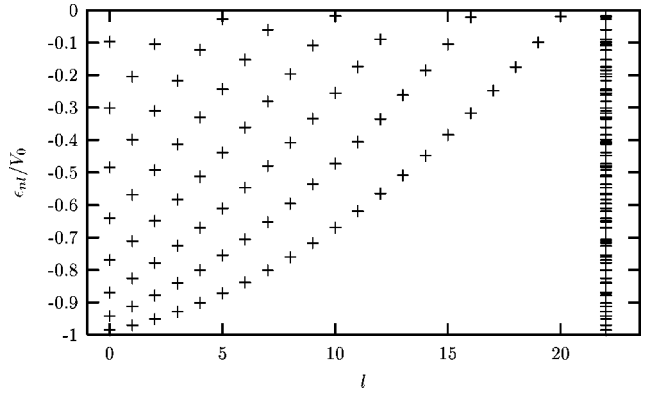

FIG. 1. Electron energy levels for a potential well such that $\kappa R\lesssim 8\pi$ (see main text). The energy spectrum at the right fails to disclose the monotonic distribution of levels as a function of l or n. Also, many states are quasidegenerate.

$$n(\mathbf{p})=\int_{-\infty}^{\infty}\frac{d\omega}{2\pi}n_{\mathrm{F}}(\omega)A(\mathbf{p},\omega), \tag{3}$$

where n_{F} is the Fermi function and A is the spectral function $A(\mathbf{p},\omega)=-2\,\mathrm{Im}\,G^R(\mathbf{p},\omega)$ (frequencies measured with respect to the chemical potential). The retarded Green's function G^R is obtained by analytic continuation from the single-particle Matsubara Green's function in frequency space, obtained from $\mathcal{G}(\mathbf{p},\tau)=-\langle T_\tau[c_{\mathbf{p}}(\tau)c_{\mathbf{p}}^\dagger(0)]\rangle$. As we shall see later on, the momentum density does not vary wildly for low momenta, but then decreases more or less steeply to zero around a value we can identify with a ''Fermi momentum.'' The width of the interval over which the electronic momentum density falls to zero, known as the broadening or smearing Δp, can be quantified from the width of the radial derivative $\partial n(p)/\partial p$. Indeed, Δp can be defined as the full width at half minimum of the pronounced, broad minimum exhibited by this function.[13] This minimum also allows us to define a Fermi momentum for the dot. For small gaps, Δp should be proportional to the HOMO-LUMO gap.

The Compton profile is the projection of the electronic momentum density onto the scattering vector. Thus if we denote by $\mathbf{q}$ the projection of the initial electron momentum onto the scattering wave vector, then the Compton profile is given by

$$J(\mathbf{q})=\int d\mathbf{p}\,n(\mathbf{p})\,\delta\left(\mathbf{p}\cdot\frac{\mathbf{q}}{q}-q\right). \tag{4}$$

In this first approach, when calculating the electron momentum density we do not consider electron-electron correlations. The noninteracting Green's function is written, in terms of our basis, $\mathcal{G}^0(\mathbf{p},\omega_n)=2\Sigma_{nlm}|\varphi_{nlm}(\mathbf{p})|^2[i\omega_n-(\epsilon_{nl}-\mu)/\hbar]^{-1}$. Thus, at zero temperature, the momentum density reduces to the expected form $n(\mathbf{p})=2\Sigma_{nlm_{\epsilon_{nl}\leqslant\epsilon_{\mathrm{F}}}}|\varphi_{nlm}(\mathbf{p})|^2$. Of course, due to rotational symmetry, one has $n=n(p)$, where p is the momentum magnitude.

B. Positron annihilation

The measurement of the Doppler-shifted positron annihilation spectrum gives information on the annihilation probability ρ as a function of the total momentum of the annihilating pair. Following Ref. 15 we define

$$\rho(\mathbf{p})=\frac{1}{(2\pi)^3}\int d\mathbf{r}d\mathbf{r}'\,e^{-i\mathbf{p}\cdot(\mathbf{r}-\mathbf{r}')}\mathcal{G}(\mathbf{r}\tau,\mathbf{r}\tau;\mathbf{r}'\tau^+,\mathbf{r}'\tau^+), \tag{5}$$

where the two-particle electron-positron Matsubara Green's function is defined by

$$\mathcal{G}(\mathbf{r}_1\tau_1,\mathbf{r}_2\tau_2;\mathbf{r}_1'\tau_1',\mathbf{r}_2'\tau_2') =\langle T_\tau[\psi(\mathbf{r}_1\tau_1)\psi_+(\mathbf{r}_2\tau_2)\psi_+^\dagger(\mathbf{r}_2'\tau_2')\psi^\dagger(\mathbf{r}_1'\tau_1')]\rangle, \tag{6}$$

where ψ and ψ_+ denote the electron and positron field operators, respectively. The definition of the Doppler profile is similar to that of the Compton profile, i.e., it is a one-dimensional projection of the annihilation probability. Thus, given a projection vector $\mathbf{q}$, one has

$$D(\mathbf{q})=\int d\mathbf{p}\rho(\mathbf{p})\,\delta\left(\mathbf{p}\cdot\frac{\mathbf{q}}{q}-q\right). \tag{7}$$

We also introduce the Doppler profile S shape parameter, which we define as

$$S=\int_{q\leqslant p_\mathrm{F}} dqD(q), \tag{8}$$

i.e., it is the fraction of annihilations with momentum $q\leqslant p_\mathrm{F}$. We note that other authors define S with other integration limits, more appropriate for the cases they are considering.[16]

The annihilation probability can be written in simple closed form assuming no electron-electron or electron-positron correlations. Indeed, in the noninteracting limit we have

$$\mathcal{G}^0(\mathbf{r}_1\tau_1,\mathbf{r}_2\tau_2;\mathbf{r}_1'\tau_1',\mathbf{r}_2'\tau_2')=\mathcal{G}^0(\mathbf{r}_1\tau_1,\mathbf{r}_1'\tau_1')\mathcal{G}_+^0(\mathbf{r}_2\tau_2,\mathbf{r}_2'\tau_2'). \tag{9}$$

Given $\mathcal{G}^0(\mathbf{r}\tau,\mathbf{r}'\tau^+)=\Sigma_{nlm\sigma}\varphi_{nlm}(\mathbf{r})\varphi_{nlm}^*(\mathbf{r}')f_{nlm\sigma}$, where f is the thermal occupation number, and a similar expression for the positron Green's function, it is readily shown that

$$\rho(\mathbf{p})=\sum_{nlm\sigma}\sum_{\nu\lambda\mu\sigma'} f_{nlm\sigma}f_{\nu\lambda\mu\sigma'} \times\left|\int d\mathbf{k}\varphi_{nlm\sigma}(\mathbf{k})\phi_{\nu\lambda\mu\sigma'}(\mathbf{p}-\mathbf{k})\right|^2, \tag{10}$$

where the Greek letters index the positron wave functions ϕ. In our case, of course, the sum over positron states reduces to one term. We point out here that, in the present approach, we suppose that the positron does not change significantly the electronic states. This amounts to saying that the neutral quasiparticle formed by the positron and its electronic cloud does not affect the remaining electronic system. This approximation has been shown to be valid in two-component density-functional theory calculations of positron annihilation in vacancies.[17]

The positron lifetime τ is the inverse of the positron total annihilation rate, which is given by

$$\lambda=\pi r_e^2 c\int d\mathbf{p}\rho(\mathbf{p}), \tag{11}$$

with r_e the classical electron radius and c the speed of light in vacuum. Given the expression for ρ in Eq. (10), it is straightforward to show that

$$\int d\mathbf{p}\rho(\mathbf{p})=\int d\mathbf{r}n(\mathbf{r})n_+(\mathbf{r}), \tag{12}$$

where $n(\mathbf{r})$ is the electron density and $n^+(\mathbf{r})$ is the positron density, so that the annihilation rate λ can be calculated in terms of the real-space wave functions. The above expression for λ is known as the independent particle model result (IPM), since it does not take into account electron-positron interaction. A more general expression, taking into account this interaction, is

$$\lambda=\pi r_e^2 c\int d\mathbf{r}n(\mathbf{r})n_+(\mathbf{r})\gamma(\mathbf{r}), \tag{13}$$

where γ is known as the enhancement factor and describes the enhanced electron density seen by the positron because of the screening cloud around it.[14]

For an inhomogeneous electron gas (HEG), the local-density approximation (LDA) of density-functional theory produces an enhancement factor, γ_0, depending only on the local electron density. Expressing the electron density n in terms of r_s [with $r_s=(3/4\pi n)^{1/3}$], the enhancement factor can be parametrized as $\gamma_0=1+1.23r_s-0.0742r_s^2+r_s^3/6$ (r_s in atomic units).[15,18] Positron lifetimes, however, are known to be underestimated in the LDA approximation.[19] A better approximation is given by the generalized gradient approximation (GGA), which attempts to take into account the nonuniformity of the electron density in an improved manner. One has[15]

$$\gamma=1+(\gamma_0-1)\exp(-\alpha\epsilon), \tag{14}$$

where α is a constant and

$$\epsilon=|\nabla n|^2/(nq_\mathrm{TF})^2, \tag{15}$$

with q_TF the local Thomas-Fermi screening length. ϵ is basically the lowest-order gradient correction to the LDA correlation hole (see Ref. 15).

III. RESULTS AND DISCUSSION

In the following, we consider quantum dots with average electron densities given by $r_s=2$–5. Also, the dot radii considered, from 10 to 25 Å, are within the range of the experimental values found in the literature.[20,21] The well depth can be calculated from $W_e=-V_0+E_\mathrm{F}$, where W_e is the work function of the material and E_F is the Fermi energy of the electrons in the dot. We take $W_e=6.62$ eV, which is the

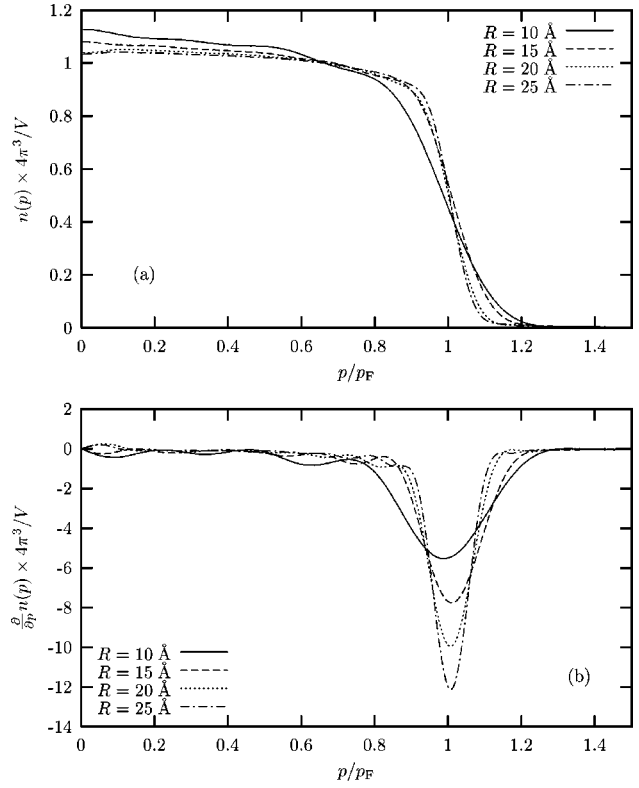

FIG. 2. (a) Electron momentum density profiles $n(p)$ par various quantum dot radii and for an electron density $r_s=3$. Profiles become more HEG-like with increasing dot radius. (b) Radial derivative of the electron momentum density profiles for the same parameter values. Clearly, the location of the minimum tends to the HEG p_F with increasing radius.

work function of CdSe,[22] a material widely used in quantum dot experiments (see Ref. 21 and references therein). To estimate V_0 we then use for E_F the HEG value corresponding to the given r_s. As we shall see later, the quantum dot Fermi level is fairly well represented by the HEG value, particularly for high electron densities. We should note that in our study all occupied l shells are completely filled (including spin degeneracy).

Let us consider first the influence of the dot radius on the electronic momentum density profile. In Fig. 2(a) we show the case of a quantum dot with an electron density $r_s=3$ and radii varying from 10 to 25 Å. In this plot, the density is normalized to the HEG density, and p_F stands for the HEG value as well. The density profile clearly tends to the expected HEG step function limit with increasing radius. The structure of the profile increases for smaller radii. We have observed that for radii smaller than, say, 5 Å, the atomiclike form of the wave functions becomes evident, particularly for low electron densities, because the electron density involves few wave functions. The departure from a step function, or broadening, around p_F is better illustrated by $\partial n(p)/\partial p$, which is shown in Fig. 2(b). One can see that the quantum dot Fermi momentum is fairly well represented by the HEG value, if we interpret the minimum of $\partial n(p)/\partial p$ as indicating the Fermi momentum of the system. The accord tends to be better for higher densities. For dots smaller than 10 Å

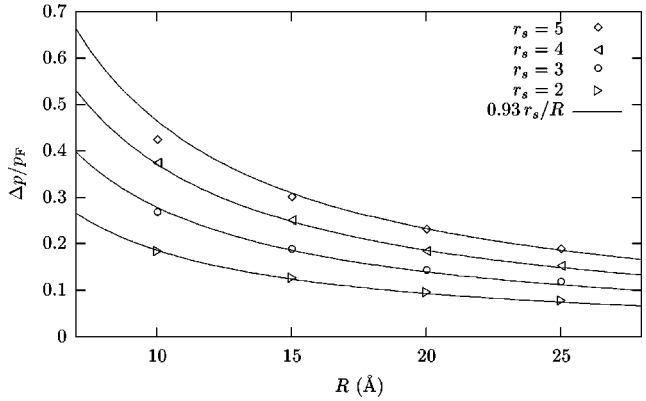

FIG. 3. The calculated broadening $\Delta p/p_F$ compared to a $0.93r_s/R$ fit. All values are reasonably well reproduced, except for low density r_s and small radius.

and lower densities, however, departures from the HEG picture are strong, and one cannot even estimate reliably the potential well depth as we did or attempt to define a Fermi momentum.

Let us look more closely at the dependence of Δp on R. For an electron gas confined to a finite volume one can expect $\Delta p\sim 1/R$. Indeed, $\Delta p\sim\Delta E_{\rm gap}/p$. But, in a finite volume $\Delta E_{\rm gap}\sim 1/R^2$ and $p\sim 1/R$. Thus $\Delta p\sim 1/R$. In Fig. 3 we have a graph of $\Delta p/p_F$ vs R for several electronic densities. The fit $\Delta p/p_F=0.93r_s/R$ represents rather well most values. In spite of the small deviations in some cases, it is quite remarkable that a single constant works so well, yielding a good scaling law. This seems to be at odds, however, with what is observed in semiconductor quantum dots,[23] where the smearing points to a more complicated $1/R^n$ behavior. It is possible that the latter results are due to lattice effects. Indeed, in a crystal, for example, near the Brillouin-zone boundary $p\sim 1/a$, where a is the lattice constant. This would give a a/R^2 dependence because then $\Delta p\sim a\Delta E_{\rm gap}$, and $E_{\rm gap}\sim 1/R^2$ as we have mentioned before. The main deviations from the fit in Fig. 3 reflect again the fact that for small radius and low density our picture tends to be less appropriate.

Let us consider now Compton profiles. Note that due to rotational symmetry, all directions for the scattering wave vector are equivalent. In Fig. 4 we show the Compton profiles for $r_s=3$ and the same dot radii considered as in Fig. 2 [the profiles are normalized so that $\int d\mathbf{p}n(\mathbf{p})=1$]. We see that the Compton profiles tend to differ more from the HEG curve for low electron density and small radius. Deviations from the HEG behavior, however, are still small in all cases. This appears to indicate that in quantum dots with a not too small density of electrons and in which lattice effects are negligible, the Compton profile is not sensitive to dot size.

We now turn our attention to positron annihilation. The positron eigenstates were determined as follows. The potential well depth seen by the positron is given by its work function $W_p=A-W_e$, where A is the positron affinity.[24] For a positron in CdSe, $A=9$ eV,[25] so that, given the electron work function value indicated above, one has $W_p=2.38$ eV. We should point out here that there is a critical

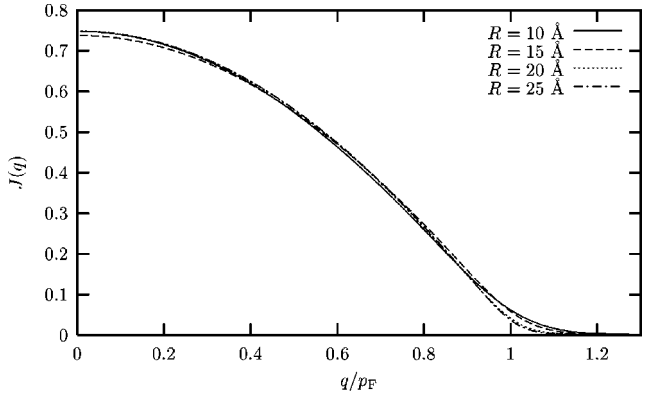

FIG. 4. Compton profiles for an electron density $r_s = 3$. The effect of dots size is more evident around the Fermi momentum, and is stronger for lower density.

dot radius below which there is no bound state for the positron. An estimate of this radius is given by $R_c = 3.068/\sqrt{W_p}$ (where the work function is in eV and the radius in Å).[26,27] In our case this yields roughly $R_c = 2$ Å, which falls below the range of radii we considered. All the following calculations were performed for the positron in its ground state. In our model, the minimum energy required to excite the positron above its ground state ranges from around 0.06 eV for a $R = 25$-Å dot to around 0.31 eV for a $R = 10$-Å dot. Temperature effects are thus negligible. In Fig. 5(a) we show the annihilation probability profiles for the parameter values considered for the electron momentum density profile in Fig. 2, i.e., $r_s = 3$ and dot radii ranging from 10 to 25 Å. The annihilation probability is normalized so that its integral over momentum space is unity. As in the case of the momentum density profile, curves tend to the HEG step function for larger dots. Compared to the momentum density profiles, the annihilation probability profiles show no structure for low momenta. This is because, for the positron in its ground state, $\rho(p)$ is essentially the convolution of the electron momentum density with the positron momentum density. The latter has a spread which is generally larger than the structure in the former, so that the convolution leaves $\rho(p)$ with an extremely weak structure away for the Fermi momentum. We also studied more closely the smearing of the annihilation probability around p_F, to see the effect of the positron. As before, we define the broadening Δp as the full width at half maximum (FWHM) of $-\partial\rho(p)/\partial p$ near p_F. We have found that the broadening still shows a $1/R$ behavior for radii $\gtrsim 15$ Å, but that it is more than 20% larger than in the case of the momentum density, with a scaling law given by $\Delta p/p_F = 1.13 r_s/R$. This is shown in Fig. 5(b). Again the values for the lowest density ($r_s = 5$) tend to comply less to the scaling law. Compared to that of the electronic momentum density, the annihilation probability broadening is larger and its deviation from a $1/R$ behavior for small dots is stronger.

In Fig. 6 we show the Doppler profiles for the different radii considered before and an electron density given by $r_s = 3$. One can see that the dot size effects are more important than for the Compton profiles. The size effects are better illustrated by the change of the shape parameter S with dot radius. The results are given in Table I, where we can see the

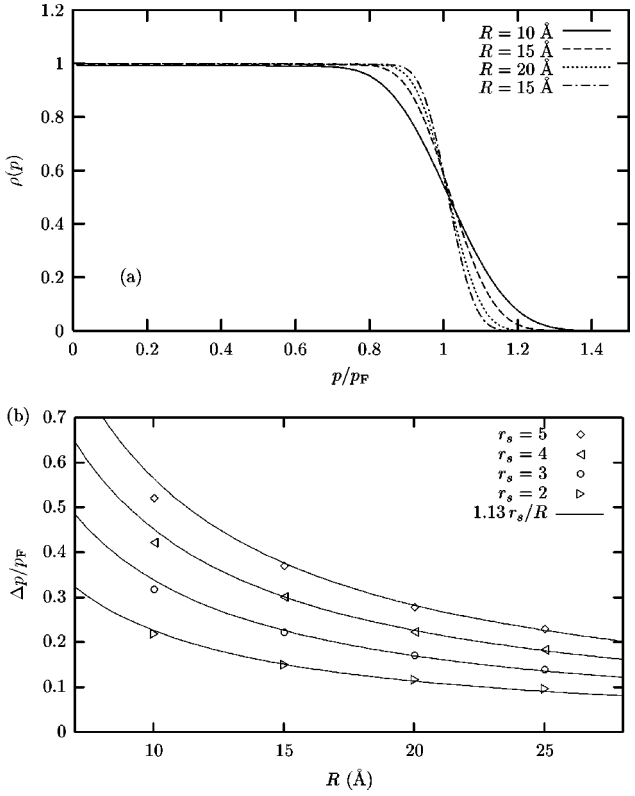

FIG. 5. (a) Positron annihilation probability as a function of momentum $\rho(p)$ for an electron density $r_s = 3$. Oscillations are very little, even for low densities and small radii, as opposed to the case of the momentum density [cf. Fig. 2(a)]. (b) The broadening $\Delta p/p_F$ of the annihilation probability as a function of R compared to a fit $1.13 r_s/R$. The positron enhances the broadening compared to the momentum density case. Though the fit is good for large radii and high densities, deviations from a $1/R$ law are stronger than in the case of the broadening of the momentum density (cf. Fig. 4).

change with electron density as well. The shape parameters are normalized to the HEG value. The values tend to 1 from below for increasing radius, as expected from Fig. 6. Also, values decrease monotonically with electron density, which implies that the annihilation probability is more broadly dis-

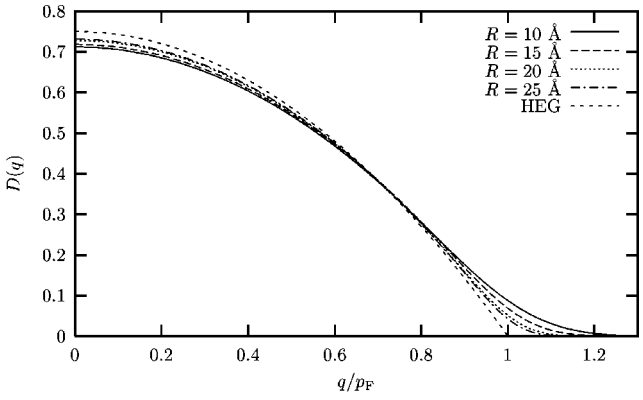

FIG. 6. Doppler profiles for the same parameter values as in Fig. 4. The size effect seem to be more important for the Doppler profile than for the Compton profile.

TABLE I. Doppler profile shape parameter normalized to the HEG value S/S_{HEG} for several electronic densities and radii. The dot radii are given in Å.

r_s	5	4	3	2
$R=10$	0.951	0.966	0.980	0.986
$R=15$	0.971	0.978	0.984	0.990
$R=20$	0.978	0.983	0.988	0.991
$R=25$	0.983	0.987	0.990	0.991

tributed for lower densities, as occurs with the momentum density. Before proceeding, let us just note the following. In Sec. II B we introduced an enhancement factor γ to take into account the electron-positron correlation when defining the annihilation rate λ. For the annihilation probability $\rho(p)$, however, this correlation is not so crucial because it does not affect its shape significantly.[15]

Let us consider, finally, positron lifetimes. In Table II we present the results for the two approximations discussed earlier for the calculation of the total annihilation rate, the LDA (enhancement factor γ_0), and the GGA [enhancement factor given by Eq. (14)]. In the latter case we should indicate that α is taken to be 0.22, which is the value for which calculated lifetimes agree with the observed values in many materials. As in the case of bulk calculations, the IPM lifetimes are much too large, and it is necessary to take into account electron-positron correlations. An interesting feature of our results is that the the lifetime behavior with radius is not monotonic. Indeed, one can see in Table II that in both cases the lifetimes tend to the HEG values for a large dot radius, although the GGA values tend more rapidly to this limit. However, if one goes toward smaller radius, lifetimes do not continue decreasing indefinitely. After reaching a minimum value for a certain radius, a lifetime will start increasing again as the radius decreases further. This is because for very small dot sizes, the positron wave function starts to spill out the dot and the electron-positron overlap starts to become smaller. Both LDA and GGA results show this trend, although the radii for which the lifetime attains its minimum are much larger in the GGA than in the LDA, particularly for low electron densities.[28] The difference between the LDA and the GGA values is smaller for larger dots, which means that for large dots both approximations tend to be equivalent, as one would expect.

IV. CONCLUSIONS

We have calculated the electronic properties of quantum dots, modeled by an electron gas confined by a spherical potential of constant depth, as seen through Compton scattering and positron annihilation studies. We find that the broadening of the electronic momentum around the Fermi momentum scales as $1/R$ for the range of quantum dot radii studied. This points to an important role played by lattice effects in semiconductor quantum dots in determining the HOMO-LUMO gap. Compton profiles are not very sensitive to the dot radius, particularly for high electron densities, except around the Fermi momentum. The broadening of the electron-positron annihilation probability around the Fermi momentum is around 20% larger than that of the electronic momentum density, but still follows a $1/R$ scaling law, though the deviations from this behavior for small dots is stronger in the latter case. Doppler profiles appear to be more sensitive to dot size than Compton profiles. Thus one can say that the positron wave function amplifies the dot size effects in this regard. The Doppler shape parameter S tends to decrease with dot size and, particularly so, with electron density, deviating increasingly from the HEG values. Finally, the positron lifetimes increase with dot size and decrease with electron density, both in the LDA and GGA approximations. As in bulk studies, the IPM results are unrealistic, with LDA and GGA giving lifetimes much closer to the values observed in different materials.[5] Our LDA and GGA results are closer to the HEG values for high electron densities ($r_s=2$ or less) and large radius. The lifetime values tend initially to decrease with radius, but after reaching a minimum for a radius that depends on the density, they increase again as the electron-positron overlap decreases for smaller radius. It would be interesting to see if this effect is detectable experimentally, particularly in metallic quantum dots, which our model suits perhaps best.

To make further progress in this area, electron-electron correlations must be taken into account. These are of course expected to have important effects on the profiles, allowing for a better description particularly in the case of low densi-

TABLE II. Positron lifetimes (ns) for the two approximations described in the text, i.e., the local-density approximation (LDA), and the generalized gradient approximation (GGA). The dot radii are given in Å.

	LDA				GGA			
r_s	5	4	3	2	5	4	3	2
$R=5$	0.3748	0.3140	0.2570	0.1491	0.4345	0.3506	0.2792	0.1559
$R=10$	0.3789	0.3268	0.2541	0.1438	0.3902	0.3337	0.2576	0.1448
$R=15$	0.3853	0.3311	0.2543	0.1451	0.3893	0.3335	0.2554	0.1454
$R=20$	0.3857	0.3350	0.2571	0.1456	0.3874	0.3361	0.2577	0.1458
$R=25$	0.3879	0.3378	0.2580	0.1460	0.3888	0.3383	0.2583	0.1461
$R=30$	0.3911	0.3386	0.2588	0.1462	0.3916	0.3390	0.2589	0.1462
HEG	0.3987	0.3463	0.2640	0.1483	0.3987	0.3463	0.2640	0.1483

ties and small dot radii. It would also be important to verify if the form of the potential well has relevant qualitative consequences. For a more detailed study of the information provided by positron annihilation in quantum dots it would be desirable to have a less *ad hoc* description of electron-positron correlations. Moreover, electrons in a quantum dot can interact with lattice vibrations and defects, which can modify strongly its electronic properties. These aspects are currently under study.

ACKNOWLEDGMENTS

This work was supported by the U.S. Department of Energy Materials Science Division under Contract No. DE-AC07-00ID13272 and U.S. Department of Energy Contract No. W-31-109-ENG-38, and benefitted from the allocation of computer time at the Northeastern University Advanced Scientific Computation Center (NU-ASCC).

*Present address: Lawrence Livermore National Laboratory, 7000 East Ave., Livermore, CA 94550-9234.

[1] See, for instance, G. Yusa and H. Sakaki, Appl. Phys. Lett. **70**, 345 (1997); P. Michler *et al.*, Science **290**, 2282 (2000); E. Dekel *et al.*, Phys. Rev. B **61**, 11009 (2000).

[2] M. Bruchez, Jr. *et al.*, Science **281**, 2013 (1998); W. Chan and S. Nie, *ibid.* **281**, 2016 (1998); M. Han, X. Gao, J. Su, and S. Nie, Nature Biotechnol. **19**, 631 (2001).

[3] See H. Drexler *et al.*, Phys. Rev. Lett. **73**, 2252 (1994); S. Tarucha *et al.*, *ibid.* **77**, 3613 (1996); N. B. Zhitenev, R. C. Ashoori, L. N. Pfeiffer, and K. W. West, *ibid.* **79**, 2308 (1997); D. Goldhaber-Gordon *et al.*, Nature (London) **391**, 156 (1998); Y. E. Kim and A. L. Zubarev, Phys. Lett. A **289**, 155 (2001).

[4] P. M. Platzman, in *Momentum Distributions*, edited by R. N. Silver and P. E. Sokol (Plenum, New York, 1989), p. 249.

[5] M. J. Puska and R. M. Nieminen, Rev. Mod. Phys. **66**, 841 (1994).

[6] M. Hakala, M. J. Puska, and R. M. Nieminen, Phys. Rev. B **57**, 7621 (1998).

[7] Y. Nagai *et al.*, Phys. Rev. B **61**, 6574 (2000); Phys. Rev. Lett. **87**, 176402 (2001).

[8] See, for instance, L. Brus, J. Phys. Chem. **90**, 2555 (1986).

[9] L. D. Landau and E. M. Lifshitz, *Relativistic Quantum Theory* (Pergamon Press, Oxford, 1971).

[10] M. Abramowitz and I. Stegun, *Handbook of Mathematical Functions* (Dover, New York, 1965).

[11] That is, for the case $\sqrt{V_0 2m/\hbar^2}R = 8\pi$.

[12] D. Davidovic and M. Tinkham, Phys. Rev. B **61**, R16359 (2000).

[13] An alternative estimation of the broadening can be obtained through the second derivative of $n(p)$. However, this tends to be numerically a less robust method in the case of the broadening of the annihilation probability, which is considered further on.

[14] T. Jarlborg and A. K. Singh, Phys. Rev. B **36**, 4660 (1987).

[15] B. Barbiellini, in *New Directions in Antimatter Chemistry and Physics*, edited by C. M. Surko and F. A. Gianturco (Kluwer Academic Publishers, Dordrecht, The Netherlands, 2001).

[16] See, e.g., Ref. 6, or R. Krause-Rehberg and H. S. Leipner, *Positron Annihilation in Semiconductors* (Springer-Verlag, Berlin, 1999), p. 21.

[17] M. J. Puska, A. P. Seitsonen, and R. M. Nieminen, Phys. Rev. B **52**, 10947 (1995).

[18] There is, in fact, a more general definition of γ_0, in which r_s is given by $n = \max(n_+, n_-)$, where n_+ and n_- are the positron and electron densities, respectively [J. Mitroy and B. Barbiellini, Phys. Rev. B **65**, 235103 (2002)]. However, n_+ could be larger than n_- in the present study only if there were very few electrons in the systems considered, which is not the case.

[19] B. Barbiellini *et al.*, Phys. Rev. B **53**, 16201 (1996).

[20] V. L. Colvin, A. P. Alivisatos, and J. G. Tobin, Phys. Rev. Lett. **66**, 2786 (1991).

[21] L. Wang and A. Zunger, Phys. Rev. B **53**, 9579 (1996).

[22] A. H. Nethercot, Phys. Rev. Lett. **33**, 1088 (1974).

[23] A. B. Denison, M. H. Weber, and K. G. Lynn (private communication).

[24] A. P. Mills, Jr., in *Positron Spectroscopy of Solids*, edited by A. Dupasquier and A. P. Mills, Jr. (IOS Press, Amsterdam, 1995), p. 209.

[25] The value of A is an estimate based on an LMTO calculation with the GGA for the electron-positron correlation; see Ref. 19.

[26] M. J. Puska, P. Lanki, and R. M. Nieminen, J. Phys.: Condens. Matter **1**, 6081 (1989).

[27] We note in passing that our values for W_p and R_c are also close to the values for positrons trapped in the Cu nanoparticles studied by Nagai *et al.* in Ref. 7.

[28] In Table II we have taken a wider range of radii to illustrate the trend more clearly. However, results for 5 Å (or lower) must be taken *cum grano salis* because for a very small radii we cannot estimate the well depth reliably from E_F and r_s. Indeed, for very small radius, the electron system does not behave like a HEG anymore.